Journal of Saudi Chemical Society (2023) **27**, 101650

King Saud University

Journal of Saudi Chemical Society

www.ksu.edu.sa
www.sciencedirect.com

ORIGINAL ARTICLE

Exploration of nonlinear optical behavior in asymmetric dithieno [3,2b:2′,3′d] pyrrole based push pull constrain: A theoretical approach

Muhammad Khalid [a,b,*], **Saira Hanif** [a,b], **Sarfraz Ahmed** [c], **Muhammad Adnan Asghar** [d], **Muhammad Imran** [e], **Ataualpa A.C. Braga** [f], **Suvash Chandra Ojha** [g,*]

[a] *Institute of Chemistry, Khwaja Fareed University of Engineering & Information Technology, Rahim Yar Khan 64200, Pakistan*
[b] *Centre for Theoretical and Computational Research, Khwaja Fareed University of Engineering & Information Technology, Rahim Yar Khan 64200, Pakistan*
[c] *Wellman Center for Photomedicine, Harvard Medical School, Massachusetts General Hospital, Boston, MA 02114, United States*
[d] *Department of Chemistry, Division of Science and Technology, University of Education Lahore, Pakistan*
[e] *Department of Chemistry, Faculty of Science, King Khalid University, P.O. Box 9004, Abha 61413, Saudi Arabia*
[f] *Departamento de Qu´ımica Fundamental, Instituto de Qu´ımica, Universidade de Saǫ Paulo, Av. Prof. Lineu Prestes, 748, Sao Paulo 05508-000, Brazil*
[g] *Department of Infectious Diseases, The Affiliated Hospital of Southwest Medical University, Luzhou 646000, China*

Received 8 March 2023; revised 29 April 2023; accepted 1 May 2023
Available online 8 May 2023

KEYWORDS

Non-fullerene;
D-π-A;
FMOs;
NLO;
NBOs;
Structural modeling

Abstract The organic compounds with end-capped acceptors obtained much consideration in optoelectronic field owing to their promising electronic properties. Herein, a series of **PTMD1-PTMD6** conjugated compounds having **D-π-A architecture** were designed *via* structural tailoring including end-capped acceptors in non-fullerene compound (**PTMR**). The **PTMR** and its designed compounds were used at M06/6-311G(d,p) level for their optimization analysis and subsequently, by using optimized geometries to perform non-linear optical (NLO), frontier molecular orbitals (FMOs) and natural bond orbitals (NBOs) analyses. The quantum chemical investigations revealed that all the designed compounds showed significant reduction in band gaps with the range of 1.467–1.880 *eV* in comparison to **PTMR** (2.308 *eV*). The band gaps were found as **PTMR** (2.308) > **PTMD6** (1.880) > **PTMD1** (1.752) > **PTMD2** (1.693) > **PTMD4** (1.532) > **PTMD5** (1.514) > **PTMD3** (1.467) with *eV* in the descending order. Further, density of states (DOS) supported the results of FMOs study, consequently, according to transition density matrix (TDMs), the designed chromophores (**PTMD1-PTMD6**) displayed the transmission of charge effectively. The **PTMD3** showed the maximum value of λ_{max} at 764.627 *nm* as compared to all the designed derivatives with greater bathochromic shift. The compound **PTMD3** showed the highest values of β_{tot} and $< \gamma >$ among all the studied compounds *i.e.*, 7.695×10^{-27} and 1.776×10^{-31} *esu*, respectively.

* Corresponding authors.
E-mail addresses: khalid@iq.usp.br (M. Khalid), suvash_ojha@swmu.edu.cn (S.C. Ojha).

https://doi.org/10.1016/j.jscs.2023.101650

According to theoretical investigation, the structural modification with different acceptor moieties played an important role in the context of desirable NLO materials for optoelectronic applications.

1. Introduction

Non-linear optics is considered as a significant subject of science which originates from laser system [1]. NLO materials have been playing a crucial role in the modern technology which fulfill the demand of NLO fields [2]. The NLO materials are greatly utilized owing to their potential applications in telecommunication, fiber-optics, electro-optics, data processing devices and information technology [3-5]. Evolution of the NLO materials have become an area of advance research in both experimental and theoretical studies [6]. In past few years, massive scientific efforts are made to produce various NLO materials including synthetic resins, molecular dyes, inorganic and organic semiconductor diodes. NLO characteristics of the organic materials are supposed to appear owing to their intermolecular charge transfer (ICT) which results in transfer of electrons from donor (D) towards acceptor (A) *via* π-spacer. The ICT through D-π-A association of NLO materials, results in stronger "push–pull" mechanism [7]. The push–pull mechanism can affect the separation of charges, amplify the asymmetric electron distribution, expand the penetration range at higher wavelengths, decrease HOMO/LUMO band gap, and enhanced the NLO response [8-10].

Various structures incorporating D-A, D-π-A, D-π-A-π-D, A-π-D-π-A, D-π-π-A, D-A-π-A and D-D-π-A are described in literature [11,12]. Furthermore, explorations of experimental and theoretical results disclosed that, strong donor "D", acceptor "A" and π-spacer moieties may improve the NLO response [13]. Subsequently, to evaluate the entire electronic properties and optical potential energy of the compounds, electronic charge density is considered as a dynamic parameter [14]. DFT is an influential tool for the analysis of dipole moment, geometry, vibrational frequency of molecular structures because of its consistency and accuracy [15]. During the last fifteen years, the consideration of researchers is shifted away from inorganic systems because organic compounds have lower dielectric coefficients and are easy to synthesize [16,17]. Owing to the high molecular susceptibility, thermal stability, appropriate refinement, intrinsic rapid reaction rates, high response time and excellent absorption co-efficient, the organic compounds are considered as required NLO materials [18,19]. A significant amount of research has been carried out to develop organic NLO materials with significant NLO properties [20,21]. To enhance the CT capacity, organic systems are linked with fullerene-based electron withdrawing groups. Fullerene-based acceptors are electron deficient molecules along with strong π-aromaticity and have 3D-conjugated structure which is used to determine the incredible NLO response, owing to greater charge delocalization and extensive π-conjugated framework [22-24]. Fullerene-based compounds have few defects such as poor photo-stability and low absorption in visible region [25].

Therefore, the interest of scientists is now moved from fullerene to non-fullerene (NF) compounds owing to their capability in modifying structures, widespread electron affinity values, facile synthesis and tunable energy levels [26]. As NF compounds displayed an excellent stability, therefore, optical and electronic characteristics of NF-based compounds can be easily modified for the sake of excellent results [27,28]. The introduction of numerous electron-deficient groups on structure of non-fullerene acceptors with prolonged π-conjugation, the NLO responses of non-fullerene chromophores have been increased. In acceptor moiety, the introduction of cyano group increases electron affinity (EA), which makes molecular surface electrostatic potential (SEP) positive and lowers the energy of LUMO [29]. The non-fullerene molecules having cyano group along with halogens at the acceptor site showed remarkable NLO behavior [30].

Herein, we took **PTIC-4Cl** as a parent compound [31] and changed it into new reference chromophore (**PTMR**). Keeping in view the above reports, NF based **PTMD1-PTMD6** have been designed by structural tailoring of **PTMR** by altering the one terminal acceptor with a powerful donor (*N,N*-dialkylaniline) and other end with different powerful electron withdrawing acceptor moieties in order to attain strong push–pull conformation [32,33]. The DFT based NLO studies for **PTMD1-PTMD6** have not been reported yet. By using computational methods, the NLO properties of the composite are examined to fulfill the research gap. For this, different computational analyses such as, maximum absorbed wavelength (λ_{max}), NBO, FMO, GRP, $\langle\alpha\rangle$, (β_{tot}) and $< \gamma >$ of reference compound and its derivatives (**PTMD1-PTMD6**) are performed. It is anticipated with great hope that all the designed compounds might effectively enhance the performance of NLO based materials in modern optical applications.

1.1. Computational procedure

To examine the NLO properties of reference compound (**PTMR**) and its derivatives (**PTMD1-PTMD6**), quantum chemical calculations were accomplished at M06/6-311G(d,p) level functional of DFT. It was reported that the M06 functional was utilized for non-covalent interactions, thermochemistry of organometallics, transition metal, nonmetals and excited states phenomena [34,35]. Further, it was also examined from literature that Pople John basis sets especially, triple zeta basis set [6-311G(d,p) (a split-valence triple-zeta basis plus d, p polarization functions on non-hydrogen and hydrogen, respectively)] [36] was significantly utilized to explore the NLO properties of organic system [37,38]. Besides these, a close harmony between experimental and DFT study was also investigated at M06 functional and 6-311G(d,p) basis set [39,40]. Therefore, these calculations had been carried out *via* Gaussian 09 package [41] in association with abovementioned level and basis set of DFT/TD-DFT in chloroform solvent whereas, visualization of the outcomes were obtained by using the Gauss View 6.0 program [42]. Among all the calculations, FMO, TDM, DOS, UV–Visible, GRPs and E_b investigations

were done at aforesaid functional and basis set in chloroform in the presence of time dependent potentials (electric and magnetic field) at TD-DFT approach to explore the excitation energies and photo absorption spectra. Nevertheless, a comparison study of absorption properties between gaseous phase and solvent phase was also performed to check the influence of media on UV–Vis properties. All other calculations like NBO, NPA and NLO were accomplished at DFT approach by utilizing above mentioned functional.

The DOS study was performed to determine the charge density of designed compounds by using PyMOlyze 2.0 program [43]. For NBO analysis, NBO 3.1 package was used by applying aforementioned level [7]. FMO analysis was performed to determine the energy gap from HOMO to LUMO [44]. Different software like Chemcraft [45], GaussSum [46], Multiwfn 3.7 [47] and Avogadro [48] were utilized for the analysis of results from output files. The dipole moment of all compounds was calculated by the given Eq. (1) [49].

$$\mu = \left(\mu_x^2 + \mu_y^2 + \mu_z^2\right)^{1/2} \quad (1)$$

The linear polarizability $< \alpha >$ was evaluated by Eq. (2) [50].

$$\langle a \rangle = 1/3\left(\alpha_{xx} + \alpha_{yy} + \alpha_{zz}\right) \quad (2)$$

With the help of Equation (3) [51] the magnitude of total first hyperpolarizability was measured.

$$\beta_{tot} = \left(\beta_x^2 + \beta_y^2 + \beta_z^2\right)\Big]^{1/2} \quad (3)$$

Where the tensors ($\beta_x = \beta_{xxx} + \beta_{xyy} + \beta_{xzz}$, $\beta_y = \beta_{yyy} + \beta_{xxy} + \beta_{yzz}$, $\beta_z = \beta_{zzz} + \beta_{xxz} + \beta_{yyz}$) were attained by using Equation (3).

The second hyperpolarizability was calculated by using Equation (4) [52].

$$< \gamma >= \sqrt{\gamma_x^2 + \gamma_y^2 + \gamma_z^2} \quad (4)$$

$$\gamma_i = \frac{1}{15}\sum_j (\gamma_{ijji} + \gamma_{ijij} + \gamma_{iijj}) i,j = \{x,y,z\} \quad (5)$$

2. Results and discussion

This research focuses on the theoretical analysis of fullerene free compounds for wide-ranging NLO outcomes. The structural modulation of the compounds is done by altering the A-π -A type configuration to D-π-A by introduction of different acceptor moieties (Scheme 1) showing a strong push–pull mechanism with larger polarity to boost the NLO features of designed compounds. The derivatives (**PTMD1-PTMD6**) contain three fragments: donor, π-linker and acceptors with greater conjugation length to increase the NLO results.

The parent chromophore (**PTIC-4Cl**) [31] has an A-π-A conformation, where hydrocarbon chains *n*-octyl (C_8H_{17}), *n*-butyl (C_4H_9), *n*-hexyl (C_6H_{13}) and ethyl (C_2H_5) used to the support spacer moieties, which are replaced with methyl (–CH_3) group to overcome computational cost. Consequently, reference compound (**PTMR**) is derived from parent compound (**PTIC-4Cl**) as shown in Fig. 1. By modifying the acceptor groups (Figure S2) in **PTIC-4Cl** a series of compounds, namely, **PTMD1-PTMD6** are designed, as illustrated in Figure S1. In all the fabricated chromophores, the π-spacer of **PTMR** and donor "D" moiety of **PTMD1** remained same. The optimized structures of studied compounds were displayed in Figure S4. The actual purpose of the current study is to design fullerene-free compounds with auspicious NLO behavior. The computations have been carried out to study HOMO/LUMO band gaps, spectral absorption analysis, polarizability $<\alpha>$, first hyperpolarizability (β_{tot}), second hyperpolarizability $< \gamma >$ and NBO analysis by DFT and TD-DFT approaches of **PTMD1-PTMD6** for the investigation of NLO properties. The compounds showed a strong push–pull mechanism with D-π-A configuration that resulted in stronger intra molecular charge transfer (ICT) properties. Tables S1-S7 illustrates the cartesian coordinates of **PTMR** and **PTMD1-PTMD6** while their IPUAC names are displayed in Table S24**.**

2.1. Electronic structures

The FMO analysis is an important approach to explore the different electronic transitions, optical behavior, chemical stability and molecular reactivity of organic systems [53]. The obtained energy gap ($E_{LUMO} - E_{HOMO}$) of investigated molecules is directly related to their kinetic and chemical stability [54]. The HOMO shows the capability of electrons donation, while LUMO demonstrates the electron accepting ability [55]. The molecules having greater E_{gap} are perceived as less reactive, more stable and chemically hard while molecules having lower E_{gap} are examined as highly reactive, less stable and soft molecules having higher polarizability and exceptional NLO response [56,57]. The energy gap (E_{gap}) sort out the efficiency of the compounds; if a compound has smaller bandgap, it shows better performance and vice versa [58]. Here, we computed the E_{gap} of investigated compounds at TD-DFT M06/6-311G(d,p) and the results are given in Table 1, while the energies of HOMO-1/LUMO + 1, and HOMO-2/LUMO + 2 are presented in Table S8.

The HOMO/LUMO energies of **PTMR** are attained to be −5.828 and −3.520 *eV*, correspondingly, with a E_{gap} value of 2.308 *eV*. The HOMO energies of **PTMD1-PTMD6** are −4.987, −4.987, −5.012, −5.008, −5.006 and −5.004, respectively, while the energies of LUMOs are collected as −3.235, −3.294, −3.545, −3.476, −3.492 and −3.124 *eV*, correspondingly. The E_{gap} of **PTMD1-PTMD6** is 1.752, 1.693, 1.467, 1.532, 1.514, and 1.880 *eV*, respectively. All of the derivatives (**PTMD1-PTMD6**) have smaller bandgaps (1.467–1.880 *eV*) than the reference chromophore (2.308 *eV*).The orbital energy gap is reduced when the A-π-A pattern is replaced with a D-π-A pattern, which encourages effective charge transfer [59].

In comparison to reference molecule, the E_{gap} has been shown to be smaller in **PTMD1-PTMD6** that may be caused by the residence of substituents (nitro, cyano and chloro) with an electron-accepting natured group in the acceptor part. In **PTMD1**, by the alteration of terminal acceptor with donor group, the energy difference in **PTMD1** is reduced to 1.752 *eV* because of strong push − pull framework from donor to acceptor. Furthermore, lessening in energy gap is detected in **PTMD2** (1.693 *eV*) when acceptor group is substituted with 2-(6,7-dichloro-2-methylene-1-oxo-1,2-dihydro-3H-benzo[b]cyclopenta[d]thiophen-3-ylidene)malononitrile (**MDM**). The compound **PTMD3** (1.467 *eV*) showed lesser band gap value than **PTMR**, which is because of presence of the acceptor (**MDP**),

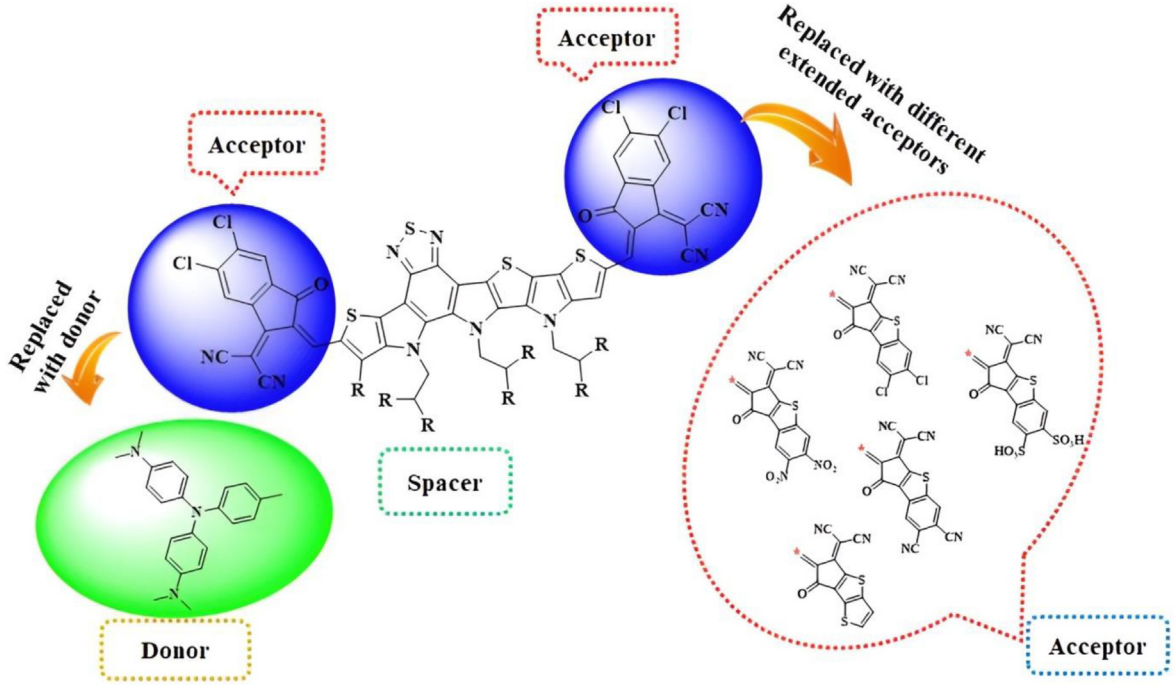

Scheme 1 The sketch map of reference and its fabricated molecules.

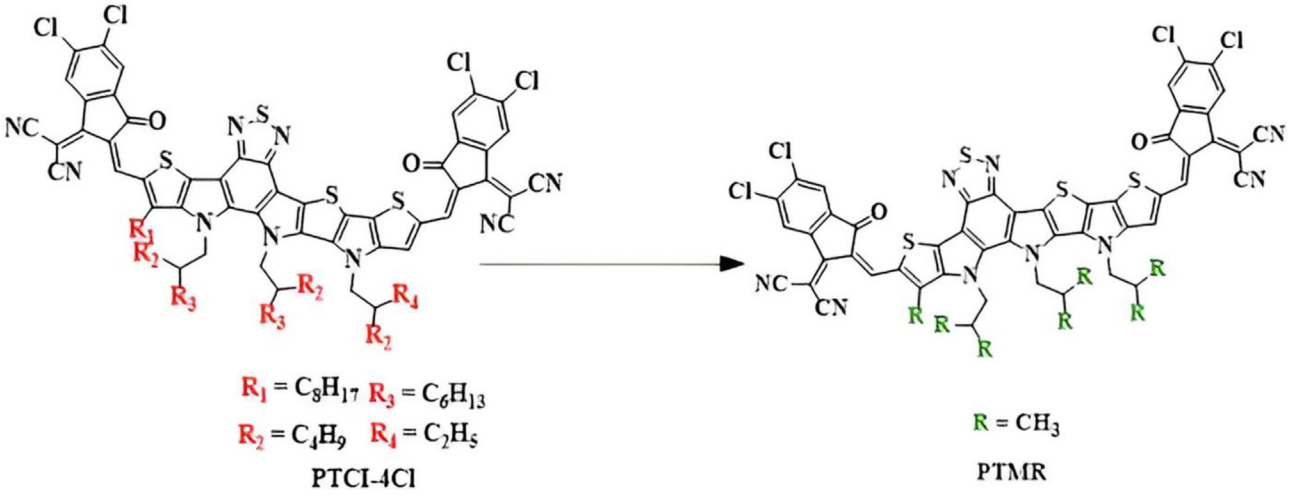

Fig. 1 Structural modifications of the parent compound (**PTCI-4Cl**) to reference compound (**PTMR**).

Table 1 Calculated FMOs energies and their energy gaps of **PTMR** and **PTMD1-PTMD6** in *eV*.

Comps	HOMO	LUMO	Δ *E* (*eV*)
PTMR	−5.828	−3.520	2.308
PTMD1	−4.987	−3.235	1.752
PTMD2	−4.987	−3.294	1.693
PTMD3	−5.012	−3.545	1.467
PTMD4	−5.008	−3.476	1.532
PTMD5	−5.006	−3.492	1.514
PTMD6	−5.004	−3.124	1.880

$\Delta E = E_{LUMO}\text{-}E_{HOMO}$.

having strongest electron withdrawing nitro unit ($-NO_2$). In **PTMD4**, the band gap (1.532 *eV*) is found greater than **PTMD3**, but lesser than reference molecule, when the $-NO_2$ unit is replaced with the SO_3H group in **MDP**. As the **MDP** acceptor is changed with **MDC** in **PTMD5**, where the $-SO_3H$ group is replaced with − CN group, the band gap is narrowed (1.514 *eV*). The **PTMD6** (1.880 *eV*) molecule has smaller energy gap than reference molecule, but greater than the compounds **PTMD2**, **PTMD3**, **PTMD4** and **PTMD5**. The decreasing order of band gap for **PTMR** and **PTMD1-PTMD6** is noted as: **PTMR > PTMD1 > PTMD2 > PTMD4 > PTMD5 > PTMD3**. **PTMD3** exhibits the lowest band gap out of all entitled structures due to improved conjugation caused by two strong electron-withdrawing $-NO_2$ units. It is found that

PTMD3 and **PTMD5** have the most efficient push–pull mechanism due to strong with **MDP** and **MDC** acceptors, respectively. For the CT, the band gap is an important factor, smaller the bandgap, higher the charge transfer rate. The counter surfaces of FMOs, showing CT from HOMO towards LUMO are illustrated in Fig. 2. and Figure S3 where charge is efficiently moves from "D" towards "A" as configuration changes from A-π-A towards D-π-A which illustrate these fabricated chromophores can be significant NLO materials.

2.2. Global reactivity parameters

The HOMO/LUMO energy values of entitled chromophores have been calculated by using TD-DFT method at aforesaid level to GRPs such as ionization potential (*IP*) [60], electron affinity (*EA*) [61], electronegativity (*X*) [62], global softness (σ) [63], global hardness (η) [64], electrophilicity index (ω) [65], and chemical potential (μ) [66]. Koopmans's Equations define these parameters [67]. The following Eqs. (5), Eq. (6) are used to determine *IP* and *EA*.

$$IP = -E_{\mathrm{HOMO}} \tag{5}$$

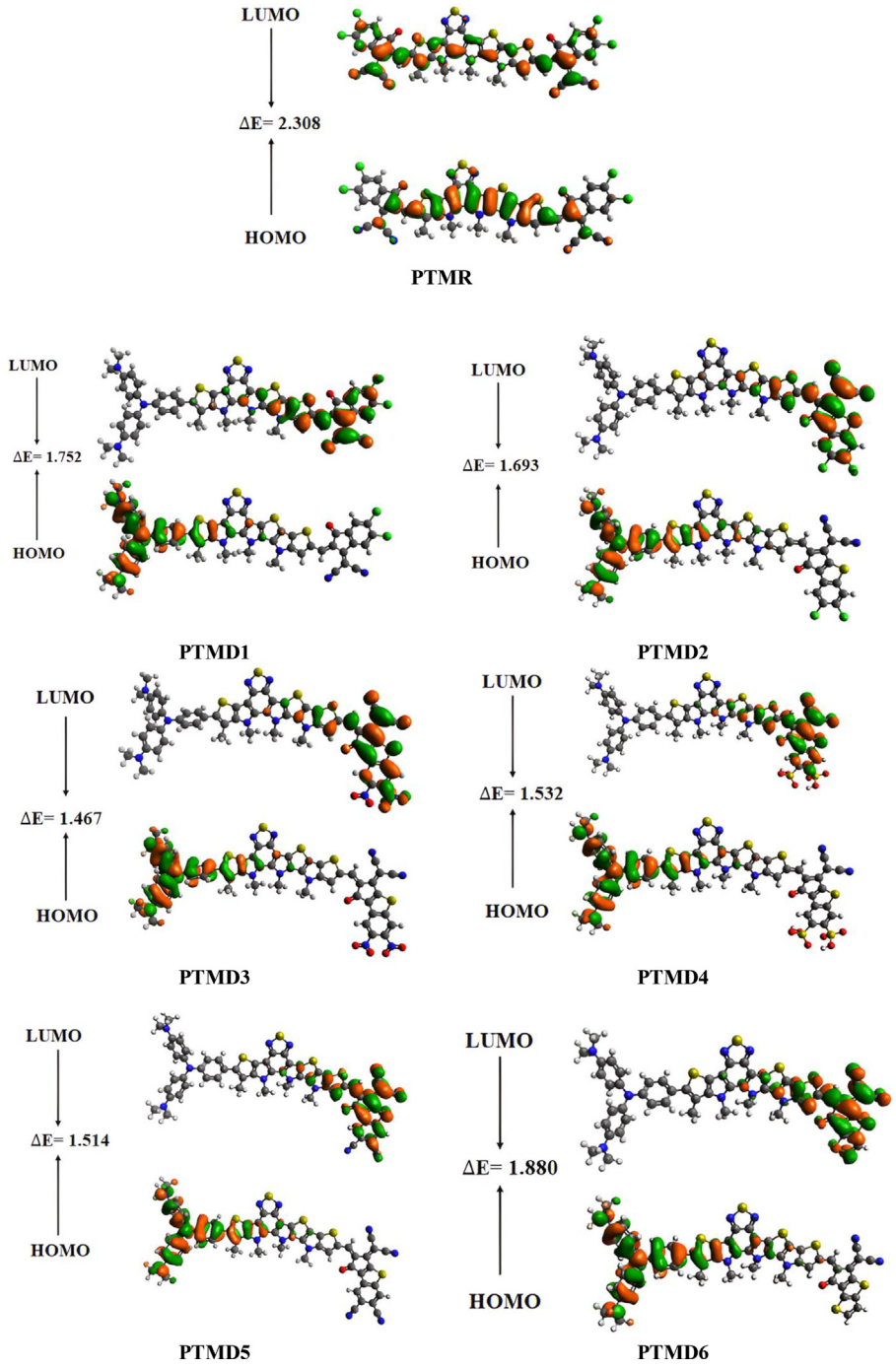

Fig. 2 Counter surfaces of FMOs of **PTMR** and **PTMD1-PTMD6**; units in *eV*.

$$EA = -E_{LUMO} \tag{6}$$

Koopmans's theorem [67] is used to analyze electronegativity (X), global hardness (η) and chemical potential (μ) as given in following Equations (7)–(9)

$$X = \frac{[IP + EA]}{2} \tag{7}$$

$$\eta = \frac{[IP - EA]}{2} \tag{8}$$

$$\mu = \frac{E_{\mathrm{HOMO}} + E_{\mathrm{LUMO}}}{2} \tag{9}$$

The electrophilicity index (ω) and global softness (σ) is calculated by following Equations as

$$\sigma = \frac{1}{2\eta} \tag{10}$$

$$\omega = \frac{\mu^2}{2\eta} \tag{11}$$

In designed derivatives (**PTMD1-PTMD6**) *IP* (5.012–4.987 *eV*) values are smaller than reference compound (5.828 *eV*), which indicate the easier discharging of electron thus, the polarization of all the molecules requires lesser amount of energy than **PTMR**. Similarly, the designed chromophore **PTMD3** has highest value of *EA* (3.545 *eV*) which shows the greater tendency to accept electron due to presence of acceptor moieties as illustrates in Table 2. The decreasing order of *EA* is **PTMD3 > PTMR > PTMD5 > PTMD4 > PTMD2 > PTMD1 > PTMD6**. Similarly, the global hardness of all the designed chromophores (**PTMD1-PTMD6**) is found to be in the range of 0.94–0.733 *eV* with greater softness values (0.682–0.532 *eV*) than the reference compound **PTMR** (η = 1.154 and σ = 0.433 *eV*), representing that, the studied compounds showed greater reactivity with high amount of polarizability, that enhanced NLO characteristics of the compounds [68]. The decreasing order of global hardness and softness is as following: **PTMR > PTMD6 > PTMD1 > PTMD2 > PTMD4 > PTMD5 > PTMD3** and **PTMD3 > PTMD5 > PTMD4 > PTMD2 > PTMD1 > PTMD6 > PTMR**, respectively (Table 2).

2.3. Density of states (DOS) analysis

DOS analysis has been accomplished to explain the electronic pattern of studied compounds (**PTMR** and **PTMD1-PTMD6**), attained by FMOs study [69]. The DOS investigation revealed the facts which are explained in the FMOs pictographs. The electronic charge distribution pattern on the molecular orbitals is determined by different acceptor moieties which can be explained by DOS percentage on HOMO-LUMO [70]. The designed compounds (**PTMD1-PTMD6**) are divided into three fragments, i.e., donor, π-spacer and acceptors as represented in graphs by red, green and blue colors, accordingly. However, **PTMR** is divided into two fragments acceptor and π-spacer having the A-π-A configuration (see Fig. 3). In this analysis, acceptor showed the electronic charge distribution pattern of 25.7, 1.1, 1.2, 1.2, 1.1, 1.2 and 1.3% to LUMO and 54.6, 65.8, 82.8, 85.1, 83.2, 84.0 and 80.9% to HOMO for **PTMR** and **PTMD1-PTMD6**, respectively. The π-spacer contributes 74.3, 14.6, 16.6, 15.1, 14.7, 15.3 and 18.5% to the LUMO and 45.4, 33.8, 17.0, 14.7, 16.6, 15.8, and 19.0% to the HOMO for **PTMR** and **PTMD1-PTMD6**. The donor contributes 84.3, 82.2, 83.7, 84.2, 83.6 and 80.2% to the LUMO and 0.3% to LUMO for **PTMD1** and 0.2% for **PTMD2-PTMD6**, respectively**.** For **PTMR**, the highest electron density is concentrated over π-spacer (green peak) for HOMO and on acceptor (red peak) for LUMO as indicated in Fig. 3. Further, from the DOS graphs, it is examined that the HOMO charge densities of all the designed compounds are mainly present on donor part and π-spacer as highest peaks of blue and green color are obtained at −5 *eV*. Similarly, in all the derivatives for LUMO maximum density is located on acceptor moieties as indicated by highest red peaks examined at −3.5 *eV* on DOS maps. Nevertheless, small electronic cloud is also study on π-spacer (green peaks) near the region of −3.5 *eV* on DOS graphs (Fig. 3). This calculation has shown that charge is efficiently transferred in all studied compounds from "D" to "A" through π-spacer.

2.4. UV–Visible analysis

Absorption spectra in UV–Visible range for **PTMR** and **PTMD1-PTMD6** in chloroform ($CHCl_3$) solvent and gaseous phase were conducted. Transition of electrons between HOMO and LUMO as well as other transitions are found in UV–Visible spectra are indicated in Table 3. Maximum absorption wavelength (λ_{max}), oscillator strength (f_{os}) and molecular transition energies of the designed compounds are depicted in Tables S9 and S10.

In chloroform solvent, maximum absorption wavelength of 764.627 *nm* is examined in the **PTMD3** with excitation energy and oscillator strength of 1.622 *eV* and 0.631, respectively,

Table 2 GRP values of compounds **PTMR** and **PTMD1-PTMD6** in *eV*.

Chromophores	*IP*	*EA*	*X*	*η*	*μ*	*ω*	*σ*
PTMR	5.828	3.520	4.674	1.154	−4.674	9.465458	0.433
PTMD1	4.987	3.235	4.111	0.876	−4.111	9.646302	0.571
PTMD2	4.987	3.294	4.141	0.847	−4.1405	10.12625	0.591
PTMD3	5.012	3.545	4.279	0.733	−4.2785	12.47823	0.682
PTMD4	5.008	3.476	4.242	0.766	−4.242	11.7458	0.653
PTMD5	5.006	3.492	4.249	0.757	−4.249	11.9247	0.661
PTMD6	5.004	3.124	4.064	0.94	−4.064	8.785157	0.532

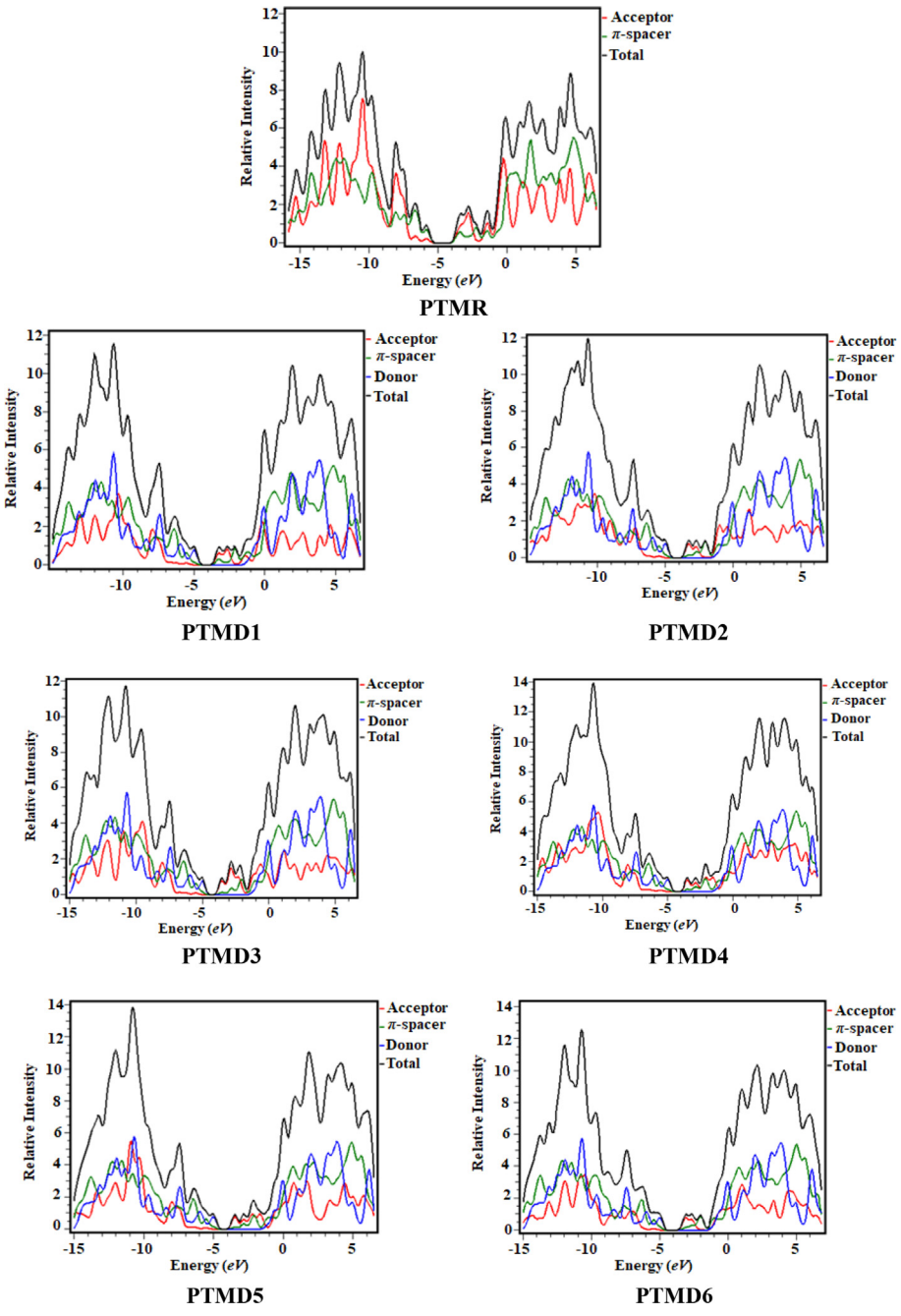

Fig. 3 DOS plots of **PTMR** and designed compounds **(PTMD1-PTMD6)**.

Table 3 Computed transition energy, wavelength (λ_{max}) and oscillator strengths in chloroform solvent.

Compounds	λ (*nm*)	E(*eV*)	f_{os}	MO Contributions
PTMR	696.540	1.780	3.302	H → L (95%), H-2 → L + 1 (2%)
PTMD1	655.862	1.890	1.439	H-1 → L (92%), H → L (4%)
PTMD2	621.568	1.995	0.851	H-1 → L + 1 (12%), H → L + 1 (84%)
PTMD3	764.627	1.622	0.631	H-1 → L (91%), H-3 → L (3%), H → L (3%)
PTMD4	553.946	2.238	0.796	H → L + 1 (89%), H-1 → L + 1 (8%)
PTMD5	553.476	2.240	0.767	H-1 → L + 1 (80%), H → L + 1 (10%), H-3 → L (2%)
PTMD6	598.322	2.072	0.912	H-1 → L + 1 (17%), H → L + 1 (78%)

which is enhanced by the presence of strongly electron capturing –NO2 group. By using electron withdrawing acceptor moieties, λ_{max} is increased in the designed compounds as illustrates in Table 3. Decreasing order of λ_{max} is obtained in the order as **PTMD3 > PTMR > PTMD1 > PTMD2 > PTMD6 > PTMD4 > PTMD5**. Minimum λ_{max} *i.e.*, hypochromic shift of 553.476 *nm* with uppermost excitation energy of 2.240 *eV* is observed in **PTMD5** because of the presence of − CN groups**.**

The absorption spectra (Fig. 4) of all entitled chromophores lie in the visible portion of the spectrum. The calculated λ_{max} (*nm*) of all the designed derivatives is noted greater in chloroform than in gaseous phase as depicted in Table S9 which might be due to solvent effect. Depending upon electronegativity of the various acceptors, the absorption spectra shift towards longer and then shorter wavelength. As the λ_{max} is increased the energy band gap is reduced. Lowest transition energy is observed in the **PTMD3** which shows superior transfer of charge from "D" to "A" because of the presence of strong electron accepting –CN and $–NO_2$ groups in the acceptor moiety. It is extracted from the above discussion that structural modeling with different efficient end groups is a successful scheme to widen the absorption range. **PTMD3** with wider absorption wavelength and lowest transition energy might prove as an efficient NLO material to be utilized in future optical applications.

2.5. Natural bond orbitals (NBOs) analysis

NBOs study explain the intra and intermolecular transitions, charge distribution and nature of bond in the designed compounds [71]. NBO study is also used to explain the transfer of charge by calculating the natural charges in D-π-A based compounds between donor and acceptor moieties [72]. Electronic charge transfer and hyperconjugation from occupied orbitals to the empty orbitals are involved in the intermolecular attractions [73]. We have accomplished the NBO study of designed compounds (**PTMD1-PTMD6**) to determine charge density and results are displayed in Table 4.

In reference compound (**PTMR**), A-π-A framework exists, whereas the studied compounds (**PTMD1-PTMD6**) have D-π-A configuration. In **PTMR**, π-spacer has the NBO charge value of 0.463, as both the acceptors are same so the charge value is −0.455, respectively. In comparison to acceptor moiety the donor has a positive value which reveals that it has an excellent ability to donate electrons. Further, the acceptors with negative value show the effective electron withdrawing capabilities. However, π-linkers have positive value which shows their ability of transfer of charge from "D" to "A" moieties without trapping. Among all studied chromophore **PTMD3** and **PTMD5** exhibited highest positive value of donors as 0.114.

By NBO 6.0 method [74] the NBO based computations are carried out at same functional by using DFT-stabilized structures. In NBO investigation, stabilization energy of compounds can be calculated by using the second-order perturbation theory with the help of given Equation [75].

$$E(2) = \Delta E_{ij} = q_i \frac{\left(F_{i,j}\right)^2}{\left(E_j - E_i\right)} \tag{12}$$

Where *i* indicate donor (D), *j* represent acceptor (A), $E^{(2)}$ means energy of stabilization, q_i and $F_{i,j}$ denotes the off-diagonal and E_i and E_j illustrate the diagonal NBO Fock matrix elements, correspondingly. NBO study was calculated by utilizing above-mentioned functional on optimized configurations of **PTMR** and **PTMD1-PTMD6** are listed in Tables S11-S17 and selected values are displayed in Table 5.

From Table 5, it is revealed that for reference compound (**PTMR**) the maximum value of π → π* occurred at 33.25 kcal/mol of π (C13-C18) → π* (C66-C67). However, least value of transition energy is calculated at 7.89 *kcal/mol* for π (C77-C81) → π* (C66-C67). Moreover, σ (C45-H47) → σ* (C32-S34) shows uppermost value of σ → σ* transition at energy of 10.24 *kcal/mol*. However, lowest value of σ (C14-C 15) → σ* (C18-C66) transition exhibits energy value of 0.5 *kcal/mol*. The maximum value of transition LP1 → π* is found at 46.37 *kcal/mol* by LP1 (N36) → π* (C11-C12). The uppermost transition of LP2 → σ* is perceived at 21.63 *kcal/-mol* by LP2 (O86) → σ* (C74-C78) as illustrated in Table 5.

For designed chromophore **(PTMD1),** highest value of transition *i.e.* π → π* is detected at 33.82 *kcal/mol* by π (C31-C32) → π* (C94-C95). However, lowest value of transition π (C13-C18) → π* (C45-C47) is noted at 7.56 *kcal/mol*

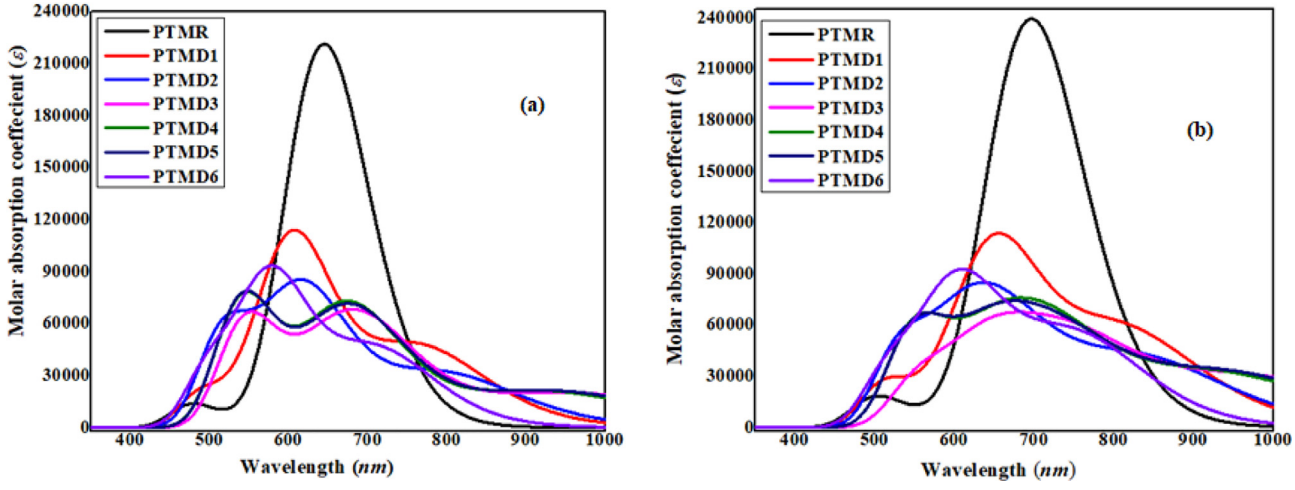

Fig. 4 UV–Visible absorption spectrum of **PTMR** and **PTMD1-PTMD6** in gas phase (a) and solvent phase (b).

Table 4 Calculated NBO charges of designed compounds (**PTMD1-PTMD6**).

Compounds	Donor	π-spacer	Acceptors
PTMD1	0.113	0.188	−0.289
PTMD2	0.111	0.117	−0.189
PTMD3	0.114	0.165	−0.279
PTMD4	0.113	0.158	−0.271
PTMD5	0.114	0.159	−0.273
PTMD6	0.104	0.093	−0.197

energy of stabilization. However, the maximum value of σ → σ* is observed at 10.55 *kcal*/*mol* by σ (C94-H96) → σ* (C32-S34). While lowest value of σ → σ* transition is detected at 0.5 *kcal*/*mol* by σ (C14-N20) → σ* (C22-H23). Moreover, topmost transition such as LP → π* is found at 46.85 *kcal*/*mol* energy by LP1 (N86) → π* (C41-C42) transition. The maximum LP → σ* value is observed at 21.63 *kcal*/*mol* by LP2 (O108) → σ* (C97-C100).

Furthermore, highest value of transition π → π* for **PTMD2** is noticed at 29.06 *kcal*/*mol* of π (C31-C32) → π* (C94-C95) transition. The lowermost value of identical transition occurs at 0.61 *kcal*/*mol* of π (C105-N106) → π* (C103-N104). Moreover, σ (N8-S9) → σ* (C3-C4) exposes maximum value of σ → σ* at energy value of 8.73 *kcal*/*mol*. However, lowest value of σ → σ* is perceived at 0.52 *kcal*/*mol* of transition σ (S107-C108) → σ* (C97-C109). The maximum value of LP → π* is found at 46.74 *kcal*/*mol* by LP1 (N36) → π* (C11-

Table 5 The selected values from NBO analysis of entitled compounds.

Compounds	Donor(*i*)	Type	Acceptor(*j*)	Type	*E*(2)[a]	*E*(J)E(i)[b]	F(i,j)[c]
PTMR	C13-C18	π	C66-C67	π*	33.25	0.3	0.09
	C77-C81	π	C66-C67	π*	7.89	0.33	0.047
	C45-H47	σ	C32-S34	σ*	10.24	0.71	0.076
	C14-C15	σ	C18-C66	σ*	0.5	1.26	0.023
	N36	LP(1)	C11-C12	π*	46.37	0.28	0.106
	O86	LP(2)	C74-C78	σ*	21.63	0.75	0.116
PTMD1	C31-C32	π	C94-C95	π*	33.82	0.31	0.091
	C13-C18	π	C45-C47	π*	7.56	0.32	0.047
	C94-H96	σ	C32-S34	σ*	10.55	0.71	0.077
	C14-N20	σ	C22-H23	σ*	0.5	1.17	0.022
	N36	LP(1)	C11-C12	π*	46.85	0.28	0.107
	O108	LP(2)	C97-C100	σ*	21.63	0.75	0.115
PTMD2	C31-C32	π	C94-C95	π*	29.06	0.31	0.085
	C105-N106	π	C103-N104	π*	0.61	0.47	0.015
	N8-S9	σ	C3-C4	σ*	8.73	1.27	0.094
	S107-C108	σ	C97-C109	σ*	0.52	1.23	0.023
	N36	LP(1)	C11-C12	π*	46.74	0.28	0.107
	O99	LP(2)	C95-C98	σ*	19.42	0.74	0.108
PTMD3	C31-C32	π	C94-C95	π*	30.77	0.3	0.086
	C103-N104	π	C105-N106	π*	0.6	0.47	0.015
	C11-C12	σ	S34-C35	σ*	9.78	0.91	0.085
	C14-N20	σ	C22-H23	σ*	0.5	1.17	0.022
	O120	LP(3)	N119-O121	π*	159.51	0.18	0.153
	O99	LP(2)	C97-C98	σ*	21.38	0.75	0.114
PTMD4	C112-C113	π	S107-C108	π*	29.25	0.2	0.08
	C103-N104	π	C105-N106	π*	0.6	0.47	0.015
	C11-C12	σ	S34-C35	σ*	9.8	0.91	0.085
	S117-O120	σ	C112-S117	σ*	0.5	1.18	0.023
	N36	LP(1)	C30-C31	π*	39.96	0.31	0.099
	O119	LP(3)	S117-O118	σ*	29.02	0.45	0.103
PTMD5	C31-C32	π	C94-C95	π*	30.57	0.3	0.086
	C98-O99	π	C94-C95	π*	3.46	0.43	0.037
	C11-C12	σ	S34-C35	σ*	9.77	0.91	0.085
	C12-S17	σ	C11-C12	σ*	0.5	1.19	0.022
	N36	LP(1)	C11-C12	π*	47.15	0.28	0.107
	O99	LP(2)	C97-C98	σ*	21.28	0.75	0.114
PTMD6	C31-C32	π	C94-C95	π*	28.17	0.31	0.084
	C98-O99	π	C97-C100	π*	4.89	0.42	0.045
	C11-C12	σ	S34-C35	σ*	9.73	0.91	0.084
	C105-N106	σ	C96-C102	σ*	0.5	1.65	0.026
	N36	LP(1)	C11-C12	π*	46.59	0.28	0.106
	O99	LP(2)	C97-C98	σ*	21.06	0.75	0.114

C12). While highest value of transition LP → σ* is found at 19.42 *kcal/mol* value of energy by LP2 (O99) → σ* (C95-C98).

For **PTMD3** compound the highest value of π → π* is observed at 30.77 *kcal/mol* by transition π (C31-C32) → π* (C94-C95). While lowest value is found at 0.6 *kcal/mol* energy value of π (C103-N104) → π* (C105-N106). However, the highest value of energy of stabilization of σ → σ* transition is found at 9.78 *kcal/mol* by σ (C11-C12) → σ* (S34-C35). The lowest value is found at 0.5 *kcal/mol* by σ (C14-N20) → σ* (C22-H23). The maximum value of LP → π* is detected at 159.51 *kcal/mol* of LP3 (O120) → π* (N119-O121). Maximum value of LP → σ* is found at 21.38 *kcal/mol* by LP2 (O99) → σ* (C97-C98) transition.

For studied compound **(PTMD4)** maximum value of transition π → π* is perceived at 29.25 *kcal/mol* of π (C112-C113) → π* (S107-C108). For same transition the lowest value of energy of stabilization is observed at 0.6 *kcal/mol* of π (C103-N104) → π* (C105-N106). Moreover, uppermost value of transition for σ → σ* transition is found at 9.8 *kcal/mol* of σ (C11-C12) → σ* (S34-C35). The lowest value of σ → σ* transition is found at 0.5 *kcal/mol* of σ (S117-O120) → σ* (C112-S117). However, LP1 (N36) → π* (C30-C31) exposes maximum value of transition LP → π* with value of 39.96 *kcal/mol*. The highest value of LP → σ* is detected at 29.02 *kcal/mol* by LP3 (O119) → σ* (S117-O118).

For compound **(PTMD5)** highest value of π → π* transition is found at 30.57 *kcal/mol* of π (C31-C32) → π* (C94-C95). However, lowest value of same transition is attained at 3.46 *kcal/mol* by π (C98-O99) → π* (C94-C95). The maximum value of σ → σ* is found at 9.77 *kcal/mol* by transition σ (C11-C12) → σ* (S34-C35). The lowest value is exposed by σ (C12-S17) → σ* (C11-C12) at 0.5 *kcal/mol* energy of stabilization. The maximum value for LP → π* is found at 47.15 *kcal/mol* by LP1 (N36) → π* (C11-C12). While highest value of the transition LP → σ* is observed at 21.28 *kcal/mol* by LP2 (O99) → σ* (C97-C98).

For **PTMD6** highest value of transition π → π* is perceived at 28.17 *kcal/mol* by π (C31-C32) → π* (C94-C95). Whereas the lowest value of is detected by π (C98-O99) → π* (C97-C100) at energy of 4.89 *kcal/mol*. However, maximum value of σ → σ* is found at 9.73 *kcal/mol* by σ (C11-C12) → σ* (S34-C35). While lowest value of σ → σ* is revealed at 0.5 *kcal/mol* by σ (C105-N106) → σ* (C96-C102). Moreover, LP1 (N36) → π* (C11-C12) exposes the highest value at energy of stabilization of 46.59 *kcal/mol*. The uppermost value of same transition is found at 21.06 *kcal/mol* by LP2 (O99) → σ* (C97-C98).

The increasing stability order of investigated compounds is noted as: **PTMD6** < **PTMD2** < **PTMD4** < **PTMD5** < **PTMR** < **PTMD1**. The designed compound **PTMD1** shows the highest stability as compared to all other designed and reference compound. Subsequently, the NBO investigation of studied compounds exposed that enrichment in hyper-conjugation and the greater ICT plays a vital role in stabilizing the studied compounds.

2.6. Transition density matrix (TDM)

TDM analysis is a significant tool to study the transfer of charge and mode of interface among acceptor, donor and π-spacer fragments in all the compounds (**PTMR** and **PTMD1-PTMD6**) [68]. The TDM of designed compounds has been computed at M06/6-311G(d,p) level of theory. TDM helps to explain the position of charge transfer within molecule and during excitation, the transitory position of electrons and holes within the molecule are determined. Due to minute effect of hydrogen atoms in electronic transition, their effect is completely neglected. The TDM heat map is 2D colored plot between number of atoms along abscissa (x-axis) and electron density distribution along y-coordinate. All the designed compounds are split into three fragments such as donor, π-linker and acceptor in order to depict the TDM properties. In TDM analysis, heat maps comprising band of colors represent the charge transfer from ground to excited state. In all the designed chromophores (**PTMD1-PTMD6**), TDM heat maps elucidate diagonal transmission of charge from electron donating to electron accepting part through π-spacer. The maximum electronic charge density is perceived at donor and significantly at acceptor and very minute at π- spacer which represents charge transfer without trapping which in turn enhance NLO response (Fig. 5).

However, in order to calculate charge shifting in studied compounds, the electron-hole coupling is also considered. In **PTMR** the hole transition is found at π-spacer part having maximum charges (0.223) as given in Figure S5. In investigated compounds *i.e.* **PTMD1**, **PTMD2**, **PTMD5** and **PTMD6** the highest electron transition is detected in "A" moiety at C59, C61, C57, O62 due to extended acceptors. In **PTMD4** and **PTMD3** two transitions are observed, in **PTMD4** both transitions are in acceptor part at C57 and C60, while in **PTMD3** the first transition is in "A" moiety whereas the second transition is in "D" part at N38 (Figure S5).

2.7. Exciton binding energy (E_b) analysis

Binding energy (E_b) is an excellent tool for the assessment of electronic properties of chromophores. Lesser the binding energy, lesser the columbic force among the hole and electron that allows for increased exciton separation in the excited state. E_b is determined by the difference of HOMO-LUMO band gap and first exciton energy, as given in Eq. (13) [76].

$$E_b = E_{H-L} - E_{opt} \tag{13}$$

The acquired results of E_b indicates that **PTMD5** chromophore can be simply separated into isolated charges and has the highest charges flow rate because of having smallest value of E_b. All designed chromophores (**PTMD1-PTMD6**) demonstrate the greater dissociation of charge and have lesser excitation E_b than **PTMR** (Table 6). The pattern of increasing binding energy for all chromophores is: **PTMD5** < **PTMD4** < **PTMD2** < **PTMD6** < **PTMD3** < **PTMD1** < **PTMR**. These results of E_b values for compounds **(PTMD1-PTMD6)** are in good agreement with TDM analysis. To summarize the findings, the compounds have lower binding energy values that support higher polarizability in chromophores which might be anticipated as appropriate constituents for utilizing them in the NLO field.

2.8. Nonlinear optical (NLO) properties

Over the last few years, significant improvements have been achieved in the field of NLO because of their numerous uses

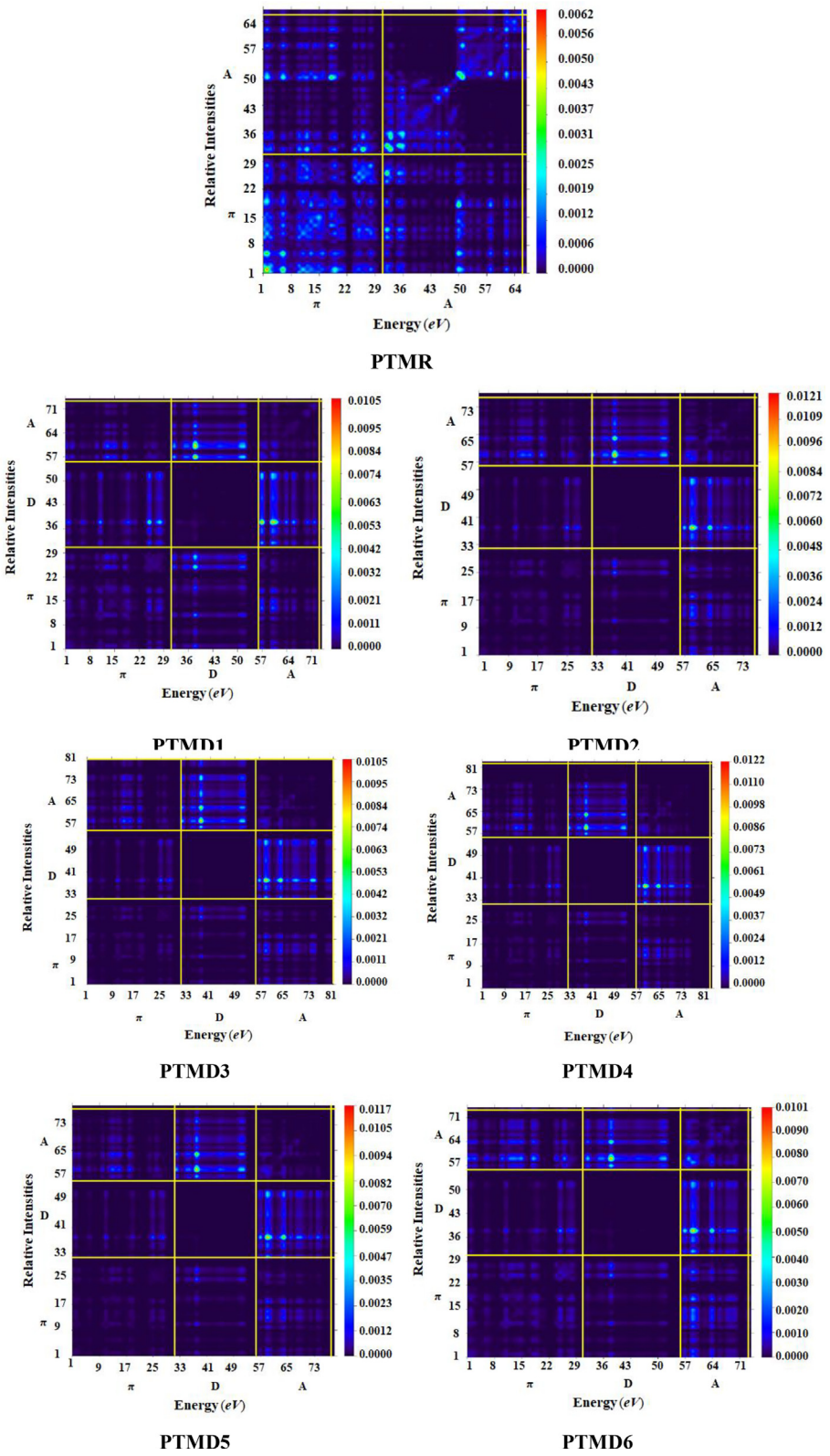

Fig. 5 TDM graphs of **PTMR** and **PTMD1-PTMD6.**

in optoelectronics [77]. Generally, organic compounds in the field of NLO materials have gained the potential improvements [78] in optical devices [79], photonic devices [80], photonic materials [81], ultrafast optical signal processing and in electrochemical sensors [82]. The root for developing NLO response in organic molecules is unsymmetrical polarization, resulting from push–pull designs of chromophore. The NLO behavior is determined by the nature of acceptor and donor

Table 6 The computed $E_{H\text{-}L}$, E_b and E_{opt} of studied compounds.

Compounds	$E_{H\text{-}L}$	E_{opt}	E_b
PTMR	2.308	1.780	0.528
PTMD1	1.752	1.890	−0.138
PTMD2	1.693	1.995	−0.302
PTMD3	1.467	1.622	−0.155
PTMD4	1.532	2.238	−0.706
PTMD5	1.514	2.240	−0.726
PTMD6	1.880	2.072	−0.192

Units in *eV*.

groups, that are linked by π-spacer [83]. The NLO parameters i.e. μ_{tot}, $\langle\alpha\rangle$, β_{tot}, and $< \gamma >$ of entitled compounds are listed in Table 7, while their respective tensors are discussed in detail in Tables S18-S23.

According to literature survey, urea is known as standard for the investigation of dipole moment and first hyper-polarizability. The dipole moment of all studied compounds is larger than that of urea molecule (1.373 D) [84]. **PTMD4** exhibited largest dipole moment (25.417 *D*) than all the investigated chromophores. However, decreasing order of dipole moment is **PTMD4** > **PTMD6** > **PTMD1** > **PTMD3** > **PTMD2** > **PTMD5** > **PTMR**. Likewise, the descending order of average linear polarizability of the designed chromophores is: **PTMD4** > **PTMD3** > **PTMD5** > **PTMR** > **PTMD2** > **PTMD1** > **PTMD6**. The modified compound **PTMD4** exhibited the topmost average polarizability value of 2.773×10^{22} *esu*. This is due to presence of two -SO_3H groups that increase electronic charge density close to acceptor moiety and enhance electron accepting capability of the compound. The linear polarizability tensor along x-axis is more dominant in **PTMR** (5.708×10^{-22} *esu*) while α_{yy} and α_{zz} are more prominent in **PTMD5** and **PTMD4** with value of 2.307×10^{-22} and 8.838×10^{-23} *esu* as shown in Table S19. According to literature survey, polarizability of molecule is affected by the Δ E between HOMO and LUMO.

The β_{tot} usually enhanced with increase in the strength of electron withdrawing substituents like chloro, nitro, cyano and fluoro groups, contributing to the nonlinear response of chromophores. Furthermore, the descending order of β_{tot} of all the designed chromophore is: **PTMD3** > **PTMD5** > **PTMD4** > **PTMD1** > **PTMD2** > **PTMD6** > **PTMR**. From all the designed chromophores, peak value of β_{tot} is found in **PTMD3** (7.695×10^{-27} *esu*) as it has strong electron with drawing units (–NO_2) than other compounds. The decrease in the value is seen in **PTMD5** (7.093×10^{-27} *esu*) when nitro group is replaced with –CN group. The $< \gamma >$ parameter shows significant role to determine the NLO behavior of compounds. Among all the designed compounds, the larger value of $< \gamma >$ is perceived in **PTMD3** and the maximum $< \gamma >$ response is examined along x-axis as presented in Table S21. Among the different tensors, γ_z showed the larger and more prominent values in **PTMD3** (8.622×10^{-35} *esu*) in contrast to other tensor components. The descending order of second order hyper-polarizability ($<\gamma>$) for designed compounds is: **PTMD3** > **PTMD5** > **PTMD4** > **PTMD1** > **PTMD2** > **PTMD6** > **PTMR**. This showed that greater charge is transferred along z-axis, which characterizes primary diagonal tensor as given in Table S21. Moreover, it can be understood from the above study that different acceptor units with π-conjugation are played an amazing role and produced NLO materials with remarkable properties. Particularly, **PTMD3** with notable NLO characteristics is the most favorable molecule to make productive NLO materials.

2.9. Natural population analysis

The NBO atomic charges play a significant role for quantum chemical study of investigated compounds. Dipole moment, electronic structure, electromagnetic spectra, and NLO properties are widely-known observables of any chemical structure that developed direct connection with the atomic charges of that organic system [1]. The charges of investigated compounds (**PTMR** and **PTMD1-PTMD6**) have been determined at abovementioned functional. The graphs of NPA are given in Figure S6.

Furthermore, it is demonstrated that, H-atoms have net positive charges, though carbon possess negative and positive charges. Nitrogen is present in **PTMR** and **PTMD1-PTMD6** and has maximum negative charge. Similarly, oxygen is also present in all entitled organic systems, contains negative charges, whereas maximum negative charge is observed at oxygen in **PTMR** and **PTMD4**. Natural population analysis is a successful strategy to obtain idea about the reactivity as all the designed compounds possess proficient charge transfer mechanism thus appeared as NLO materials.

3. Conclusion

Herein, a series of chromophores (**PTMD1-PTMD6**) have been designed *via* utilizing *N*, *N*-dialkylaniline as a donor moiety having auspicious properties of electron donation and fixed π-spacer along with different acceptor units in reference com-

Table 7 Investigated μ_{tot}, $\langle\alpha\rangle$, β_{tot} and $< \gamma >$ values of designed compounds.

Compounds	μ_{tot}	$\langle\alpha\rangle \times 10^{-22}$	$\beta_{tot} \times 10^{-27}$	$<\gamma> \times 10^{-32}$
PTMR	2.410	2.679	0.685	4.331
PTMD1	22.886	2.618	5.791	9.770
PTMD2	21.627	2.629	4.947	8.430
PTMD3	21.889	2.772	7.695	17.76
PTMD4	25.417	2.773	6.758	13.81
PTMD5	21.267	2.763	7.093	15.13
PTMD6	23.469	2.463	3.689	5.160

μ units are in *D*, $\langle\alpha\rangle$, β_{tot} and $< \gamma >$ units are in *esu*.

pound (**PTMR**). The prospective of this research was to communicate the NLO response ($<\alpha>$, β_{tot} and $<\gamma>$) of **PTMD1-PTMD6.** The ΔE order is attained as **PTMR > PTMD1 > PTMD2 > PTMD4 > PTMD5 > PTMD3**. In UV–Vis spectra, the maximum absorption wavelength i.e. 764.627 *nm* is examined in **PTMD3** with 1.622 eV and 0.631 values of excitation energy and oscillator strength, respectively. The results of E_b revealed that, **PTMD5** can be easily separated into isolated charges because of lowest binding energy value. The values of $<\alpha>$, β_{tot} and $<\gamma>$ are obtained to be higher for designed compounds than **PTMR**. Among designed ones, the compound (**PTMD3**) shows the greater values of β_{tot} and $<\gamma>$ (7.695×10^{-27} and 1.776×10^{-31} *esu*). In contrast to urea the designed compounds showed remarkable NLO response. The development of D-π-A compounds having donor and acceptor terminals may lead to the significant role in NLO materials. Furthermore, from the preceding discussion it is derived that tailored D-π-A based compound might exhibit excellent properties in NLO field. These findings of **PTMD1-PTMD6** may contribute comprehensive insights in NLO based research.

CRediT authorship contribution statement

Muhammad Khalid: Methodology, Software, Project administration. **Saira Hanif:** Conceptualization, Methodology. **Sarfraz Ahmed:** Conceptualization, Methodology, Software. **Muhammad Adnan Asghar:** Data curation, Formal analysis. **Muhammad Imran:** Conceptualization, Resources. **Ataualpa A.C. Braga:** Data curation, Formal analysis, Validation. **Suvash Chandra Ojha:** Conceptualization, Methodology, Software.

Declaration of Competing Interest

The authors declare that they have no known competing financial interests or personal relationships that could have appeared to influence the work reported in this paper.

Acknowledgements

Dr. Muhammad Khalid gratefully acknowledges the financial support of HEC Pakistan (project no. 20-14703/NRPU/R&D/HEC/2021). A.A.C.B. (grant 2015/01491-3) is highly thankful to Fundação de Amparo à Pesquisa do Estado de São Paulo for the cooperation and financial assistance. A.A.C.B. (grant 312550/2020-0) also thanks to the Brazilian National Research Council (CNPq) for financial support and fellowship. MI expresses appreciation to the Deanship of Scientific Research at King Khalid University Saudi Arabia through the research groups program under Grant Number R.G.P. 2/256/44. SCO acknowledges the support from the doctoral research fund of the Affiliated Hospital of Southwest Medical University.

Appendix A. Supplementary material

Supplementary data to this article can be found online at https://doi.org/10.1016/j.jscs.2023.101650.

References

[1] V. Muttannavar, R.M. Melavanki, P. Bhavya, R. Kusanur, N. R. Patil, L.R. Naik, Non-linear optical properties study of two heterocyclic compounds, Int. J. Life Sci. Pharma Res. 8 (2018) 24–30.

[2] S. Kumar, S. Muhammad, J. Koh, M. Khalid, K. Ayub, A combined experimental and computational study of 2, 2'-(diazene-1, 2-diylbis (4, 1-phenylene)) bis (6-(butylamino)-1H-benzo [de] isoquinoline-1, 3 (2H)-dione): Synthesis, optical and nonlinear optical properties, Optik 192 (2019) 162952.

[3] B. Mohan, M. Choudhary, G. Kumar, S. Muhammad, N. Das, K. Singh, A.G. Al-Sehemi, S. Kumar, An experimental and computational study of pyrimidine based bis-uracil derivatives as efficient candidates for optical, nonlinear optical, and drug discovery applications, Synthetic Commun. 50 (2020) 2199–2225.

[4] S. Muhammad, S. Hussain, X. Chen, A.G. Al-Sehemi, Z.-J. Li, C.-H. Lai, J. Iqbal, A dual approach to study the synthesis, crystal structure and nonlinear optical properties of binuclear Pd (II) complex of 3-methyl-5-(trifluoromethyl) pyrazole and its potential quantum chemical analogues, Inorg. Chim. Acta 494 (2019) 160–167.

[5] L. Chen, G. Yu, W. Chen, C. Tu, X. Zhao, X. Huang, Constructing a mixed π-conjugated bridge to effectively enhance the nonlinear optical response in the Möbius cyclacene-based systems, PCCP 16 (2014) 10933–10942.

[6] M. Akram, M. Adeel, M. Khalid, M.N. Tahir, M.U. Khan, M. A. Asghar, M.A. Ullah, M. Iqbal, A combined experimental and computational study of 3-bromo-5-(2, 5-difluorophenyl) pyridine and 3, 5-bis (naphthalen-1-yl) pyridine: Insight into the synthesis, spectroscopic, single crystal XRD, electronic, nonlinear optical and biological properties, J. Mol. Struct. 1160 (2018) 129–141.

[7] M. Khalid, H.M. Lodhi, M.U. Khan, M. Imran, Structural parameter-modulated nonlinear optical amplitude of acceptor–π–D–π–donor-configured pyrene derivatives: a DFT approach, RSC Adv. 11 (2021) 14237–14250.

[8] M. Haroon, R. Mahmood, M.R.S.A. Janjua, An interesting behavior and Nonlinear Optical (NLO) response of hexamolybdate metal cluster: theoretical insight into electro-optic modulation of hybrid composites, J. Clust. Sci. 28 (2017) 2693–2708.

[9] M.R.S.A. Janjua, Z.-M. Su, W. Guan, C.-G. Liu, L.-K. Yan, P. Song, G. Maheen, Tuning second-order non-linear (NLO) optical response of organoimido-substituted hexamolybdates through halogens: Quantum design of novel organic-inorganic hybrid NLO materials, Aust. J. Chem. 63 (2010) 836–844.

[10] M.R.S.A. Janjua, S. Jamil, A. Mahmood, A. Zafar, M. Haroon, H.N. Bhatti, Solvent-dependent non-linear optical properties of 5, 5′-disubstituted-2, 2′-bipyridine complexes of ruthenium (II): a quantum chemical perspective, Aust. J. Chem. 68 (2015) 1502–1507.

[11] M.U. Khan, M. Ibrahim, M. Khalid, M.S. Qureshi, T. Gulzar, K.M. Zia, A.A. Al-Saadi, M.R.S.A. Janjua, First theoretical probe for efficient enhancement of nonlinear optical properties of quinacridone based compounds through various modifications, Chem. Phys. Lett. 715 (2019) 222–230.

[12] I. Khan, M. Khalid, M. Adeel, S.I. Niaz, I. Shafiq, S. Muhammad, A.A.C. Braga, Palladium-catalyzed synthesis of 5-(arylated) pyrimidines, their characterization, electronic communication, and non-linear optical evaluations, J. Mol. Struct. 1237 (2021) 130408.

[13] R. Canton-Vitoria, Y. Sayed-Ahmad-Baraza, M. Pelaez-Fernandez, R. Arenal, C. Bittencourt, C.P. Ewels, N. Tagmatarchis, Functionalization of MoS2 with 1, 2-dithiolanes: toward donor-acceptor nanohybrids for energy conversion, Npj 2D Mater. Appl. 1 (2017) 1–9.

[14] A. Mahmood, S.-U.-D. Khan, U.A. Rana, M.R.S.A. Janjua, M. H. Tahir, M.F. Nazar, Y. Song, Effect of thiophene rings on UV/visible spectra and non-linear optical (NLO) properties of triphenylamine based dyes: a quantum chemical perspective, J. Phys. Org. Chem. 28 (2015) 418–422.

[15] S. Grimme, J. Antony, S. Ehrlich, H. Krieg, A consistent and accurate ab initio parametrization of density functional dispersion correction (DFT-D) for the 94 elements H-Pu, J. Chem. Phys. 132 (2010) 154104.
[16] Y. Wang, W. Tam, S.H. Stevenson, R.A. Clement, J. Calabrese, New organic non-linear optical materials of stilbene and diphenylacetylene derivatives, Chem. Phys. Lett. 148 (1988) 136–141.
[17] Z. Yuan, N.J. Taylor, Y. Sun, T.B. Marder, I.D. Williams, C. Lap-Tak, Synthesis and second-order nonlinear optical properties of three coordinate organoboranes with diphenylphosphino and ferrocenyl groups as electron donors: crystal and molecular structures of (E)-D CH CH B (mes) 2 and D C C B (mes) 2 [D P (C6H52,(η-C5H5) Fe (η-C5H4); mes = 2, 4, 6-(CH3) 3C6H2], J. Organomet. Chem. 449 (1993) 27–37.
[18] D.J. Williams, Organic polymeric and non-polymeric materials with large optical nonlinearities, Angew. Chem. Int. Ed. Eng. 23 (1984) 690–703.
[19] W.E. Moerner, S.M. Silence, Polymeric photorefractive materials, Chem. Rev. 94 (1994) 127–155.
[20] A. Elmali, A. Karakaş, H. Ünver, Nonlinear optical properties of bis [(p-bromophenyl-salicylaldiminato) chloro] iron (III) and its ligand N-(4-bromo)-salicylaldimine, Chem. Phys. 309 (2005) 251–257.
[21] A. Irfan, M. Pannipara, A.G. Al-Sehemi, M.W. Mumtaz, M.A. Assiri, A.R. Chaudhry, S. Muhammad, Exploring the effect of electron withdrawing groups on optoelectronic properties of pyrazole derivatives as efficient donor and acceptor materials for photovoltaic devices, Z. Phys. Chem. 233 (2019) 1625–1644.
[22] D.M. Guldi, Fullerenes: three dimensional electron acceptor materials, Chem. Commun. 321–327 (2000).
[23] Y. He, Y. Li, Fullerene derivative acceptors for high performance polymer solar cells, PCCP 13 (2011) 1970–1983.
[24] S. Couris, E. Koudoumas, A.A. Ruth, S. Leach, Concentration and wavelength dependence of the effective third-order susceptibility and optical limiting of C60 in toluene solution, J. Phys. B Atomic Mol. Phys. 28 (1995) 4537.
[25] A. Wadsworth, M. Moser, A. Marks, M.S. Little, N. Gasparini, C.J. Brabec, D. Baran, I. McCulloch, Critical review of the molecular design progress in non-fullerene electron acceptors towards commercially viable organic solar cells, Chem. Soc. Rev. 48 (2019) 1596–1625.
[26] M.N. Arshad, I. Shafiq, M. Khalid, A.M. Asiri, Exploration of the Intriguing Photovoltaic Behavior for Fused Indacenodithiophene-Based A-D–A Conjugated Systems: a DFT Model Study, ACS Omega 7 (2022) 11606–11617.
[27] A. Mahmood, A. Irfan, J.-L. Wang, Machine learning and molecular dynamics simulation-assisted evolutionary design and discovery pipeline to screen efficient small molecule acceptors for PTB7-Th-based organic solar cells with over 15% efficiency, J. Mater. Chem. A 10 (2022) 4170–4180.
[28] P. Cheng, G. Li, X. Zhan, Y. Yang, Next-generation organic photovoltaics based on non-fullerene acceptors, Nat. Photonics 12 (2018) 131–142.
[29] C. Yao, Y. Yang, L. Li, M. Bo, J. Zhang, C. Peng, Z. Huang, J. Wang, Elucidating the key role of the cyano (- C$\equiv$ N) group to construct environmentally friendly fused-ring electron acceptors, J. Phys. Chem. C 124 (2020) 23059–23068.
[30] C. Yao, Y. Yang, L. Li, M. Bo, C. Peng, J. Wang, Quad-rotor-shaped non-fullerene electron acceptor materials with potential to enhance the photoelectric performance of organic solar cells, J. Mater. Chem. A 7 (2019) 18150–18157.
[31] Z. Xia, J. Zhang, X. Gao, W. Song, J. Ge, L. Xie, X. Zhang, Z. Liu, Z. Ge, Fine-Tuning the Dipole Moment of Asymmetric Non-Fullerene Acceptors Enabling Efficient and Stable Organic Solar Cells, ACS Appl. Mater. Interfaces 13 (2021) 23983–23992.
[32] H. Kang, A. Facchetti, P. Zhu, H. Jiang, Y. Yang, E. Cariati, S. Righetto, R. Ugo, C. Zuccaccia, A. Macchioni, Exceptional Molecular Hyperpolarizabilities in Twisted π-Electron System Chromophores, Angew. Chem. Int. Ed. 44 (2005) 7922–7925.
[33] S. Aithal, P.S. Aithal, G. Bhat, Literature review on organic materials for third harmonic optical and photonic applications, Int. J. Adv. Trends Eng. Technol. (IJATET). 1 (2016) 151–162.
[34] M. Khalid, A. Ali, M.F.U. Rehman, M. Mustaqeem, S. Ali, M. U. Khan, S. Asim, N. Ahmad, M. Saleem, Exploration of noncovalent interactions, chemical reactivity, and nonlinear optical properties of piperidone derivatives: a concise theoretical approach, ACS Omega 5 (2020) 13236–13249.
[35] Y. Zhao, D.G. Truhlar, The M06 suite of density functionals for main group thermochemistry, thermochemical kinetics, noncovalent interactions, excited states, and transition elements: two new functionals and systematic testing of four M06-class functionals and 12 other functionals, Theor. Chem. Acc. 120 (2008) 215–241.
[36] R. Poirier, R. Kari, I.G. Csizmadia, Handbook of Gaussian basis sets (1985).
[37] D. Avci, A. Başoğlu, Y. Atalay, Effects of different basis sets and donor-acceptor groups on linear and second-order nonlinear optical properties and molecular frontier orbital energies, Int. J. Quantum Chem 111 (2011) 130–147.
[38] D. Paschoal, M.F. Costa, H.F. Dos Santos, NLO-X (X = I-III): New Gaussian basis sets for prediction of linear and nonlinear electric properties, Int. J. Quantum Chem 114 (2014) 796–804.
[39] M. Haroon, T. Akhtar, M. Khalid, H. Mehmood, M.A. Asghar, R. Baby, R. Orfali, S. Perveen, Synthesis, characterization and exploration of photovoltaic behavior of hydrazide based scaffolds: a concise experimental and DFT study, RSC Adv. 13 (2023) 7237–7249.
[40] W.A. Siddiqui, M. Khalid, A. Ashraf, I. Shafiq, M. Parvez, M. Imran, A. Irfan, M. Hanif, M.U. Khan, F. Sher, Antibacterial metal complexes of o-sulfamoylbenzoic acid: synthesis, characterization, and DFT study, Appl. Organomet. Chem. 36 (2022) e6464.
[41] M.J. Frisch, F.R. Clemente, Gaussian 09, revision a. 01, mj frisch, gw trucks, hb schlegel, ge scuseria, ma robb, jr cheeseman, g, Scalmani, V. Barone, B. Mennucci, GA Petersson, H. Nakatsuji, M. Caricato, X. Li, HP Hratchian, AF Izmaylov, J. Bloino, G. Zhe. (2009) 20–44.
[42] R.A. Shehzad, J. Iqbal, M.U. Khan, R. Hussain, H.M.A. Javed, A. ur Rehman, M.U. Alvi, M. Khalid, Designing of benzothiazole based non-fullerene acceptor (NFA) molecules for highly efficient organic solar cells, Comput. Theor. Chem. 1181 (2020) 112833.
[43] N.M. O'boyle, A.L. Tenderholt, K.M. Langner, Cclib: a library for package-independent computational chemistry algorithms, J. Comput. Chem. 29 (2008) 839–845.
[44] M.U. Khan, M. Khalid, I. Shafiq, R.A. Khera, Z. Shafiq, R. Jawaria, M. Shafiq, M.M. Alam, A.A.C. Braga, M. Imran, Theoretical investigation of nonlinear optical behavior for rod and T-Shaped phenothiazine based D-π-A organic compounds and their derivatives, J. Saudi Chem. Soc. 25 (2021) 101339.
[45] G.A. Zhurko, D.A. Zhurko, ChemCraft, version 1.6, URL: Http://Www, Chemcraftprog. Com. (2009).
[46] N.M. O'boyle, A.L. Tenderholt, K.M. Langner, J. Comput. Chem. 29 (2008) 839–845.
[47] T. Lu, F. Chen, Multiwfn: a multifunctional wavefunction analyzer, J. Comput. Chem. 33 (2012) 580–592.
[48] M.D. Hanwell, D.E. Curtis, D.C. Lonie, T. Vandermeersch, E. Zurek, G.R. Hutchison, Avogadro: an advanced semantic chemical editor, visualization, and analysis platform, J. Cheminformatics 4 (2012) 1–17.
[49] L. Kara Zaitri, S.M. Mekelleche, Computational study of linear and nonlinear optical properties of substituted thiophene imino

dyes using long-range corrected hybrid DFT methods, Mol. Phys. 118 (2020) 1618508.
[50] A. Alparone, Linear and nonlinear optical properties of nucleic acid bases, Chem. Phys. 410 (2013) 90–98.
[51] A. Plaquet, M. Guillaume, B. Champagne, F. Castet, L. Ducasse, J.-L. Pozzo, V. Rodriguez, In silico optimization of merocyanine-spiropyran compounds as second-order nonlinear optical molecular switches, PCCP 10 (2008) 6223–6232.
[52] K.B. Lipkowitz, D.B. Boyd, Three-Dimensional Structure Database Searches, Rev. Comput. Chem. 7 (7) (2009) 67.
[53] M. Khalid, M. Zafar, S. Hussain, M.A. Asghar, R.A. Khera, M. Imran, F.L. Abookleesh, M.Y. Akram, A. Ullah, Influence of end-capped modifications in the nonlinear optical amplitude of nonfullerene-based chromophores with a D- π–A architecture: a DFT/TDDFT Study, ACS Omega 7 (2022) 23532–23548.
[54] P. Ferdowsi, Y. Saygili, W. Zhang, T. Edvinson, L. Kavan, J. Mokhtari, S.M. Zakeeruddin, M. Grätzel, A. Hagfeldt, Molecular design of efficient organic D-A—-A dye featuring triphenylamine as donor fragment for application in dye-sensitized solar cells, ChemSusChem 11 (2018) 494–502.
[55] M. Khalid, M. Ali, M. Aslam, S.H. Sumrra, M.U. Khan, N. Raza, N. Kumar, M. Imran, Frontier molecular, Natural bond orbital, UV-Vis spectral stduy, Solvent influence on geometric parameters, Vibrational frequencies and solvation energies of 8-Hydroxyquinoline, Int. J. Pharm. Sci. Res. 8 (2017) 13040.
[56] M. Khalid, M.U. Khan, I. Shafiq, R. Hussain, K. Mahmood, A. Hussain, R. Jawaria, A. Hussain, M. Imran, M.A. Assiri, NLO potential exploration for D–π–A heterocyclic organic compounds by incorporation of various π-linkers and acceptor units, Arab. J. Chem. 14 (2021) 103295.
[57] M. Khalid, M.U. Khan, I. Shafiq, R. Hussain, A. Ali, M. Imran, A.A. Braga, M. Fayyaz ur Rehman, M.S. Akram, Structural modulation of π-conjugated linkers in D–π–A dyes based on triphenylamine dicyanovinylene framework to explore the NLO properties, Royal Society Open, Science 8 (2021) 210570.
[58] T. Hassan, R. Hussain, M.U. Khan, U. Habiba, Z. Irshad, M. Adnan, J. Lim, Development of non-fused acceptor materials with 3D-Interpenetrated structure for stable and efficient organic solar cells, Mater. Sci. Semicond. Process. 151 (2022) 107010.
[59] C. Jiao, Z. Guo, B. Sun, L. Meng, X. Wan, M. Zhang, H. Zhang, C. Li, Y. Chen, An acceptor–donor–acceptor type non-fullerene acceptor with an asymmetric backbone for high performance organic solar cells, J. Mater. Chem. C 8 (2020) 6293–6298.
[60] R.G. Parr, W. Yang, Density functional approach to the frontier-electron theory of chemical reactivity, J. Am. Chem. Soc. 106 (1984) 4049–4050.
[61] R.G. Parr, R.A. Donnelly, M. Levy, W.E. Palke, Electronegativity: the density functional viewpoint, J. Chem. Phys. 68 (1978) 3801–3807.
[62] R.G. Pearson, Absolute electronegativity and absolute hardness of Lewis acids and bases, J. Am. Chem. Soc. 107 (1985) 6801–6806.
[63] R. Parthasarathi, J. Padmanabhan, M. Elango, V. Subramanian, P.K. Chattaraj, Intermolecular reactivity through the generalized philicity concept, Chem. Phys. Lett. 394 (2004) 225–230.
[64] R.G. Parr, R.G. Pearson, Absolute hardness: companion parameter to absolute electronegativity, J. Am. Chem. Soc. 105 (1983) 7512–7516.
[65] P.K. Chattaraj, D.R. Roy, Update 1 of: electrophilicity index, Chemical Reviews. 107 (2007) PR46–PR74.
[66] P. Politzer, D.G. Truhlar, Chemical applications of atomic and molecular electrostatic potentials: reactivity, structure, scattering, and energetics of organic, inorganic, and biological systems, Springer Science & Business Media, 2013.
[67] T. Koopmans, Ordering of wave functions and eigenenergies to the individual electrons of an atom, Physica 1 (1933) 104–113.
[68] M. Khalid, M.N. Arshad, S. Murtaza, I. Shafiq, M. Haroon, A. M. Asiri, S.F. de AlcântaraMorais, A.A. Braga, Enriching NLO efficacy via designing non-fullerene molecules with the modification of acceptor moieties into ICIF2F: an emerging theoretical approach, RSC Adv. 12 (2022) 13412–13427.
[69] M. Khalid, I. Shafiq, M. Zhu, M.U. Khan, Z. Shafiq, J. Iqbal, M.M. Alam, A.A.C. Braga, M. Imran, Efficient tuning of small acceptor chromophores with A1-π-A2-π-A1 configuration for high efficacy of organic solar cells via end group manipulation, J. Saudi Chem. Soc. 25 (2021) 101305.
[70] H. Lin, Q. Wang, Non-fullerene small molecule electron acceptors for high-performance organic solar cells, J. Energy Chem. 27 (2018) 990–1016.
[71] F. Weinhold, C.R. Landis, Natural bond orbitals and extensions of localized bonding concepts, Chemistry Educ. Res. Pract. 2 (2001) 91–104.
[72] M.N. Arshad, M. Khalid, M. Asad, A.M. Asiri, M.M. Alotaibi, A.A. Braga, A. Khan, Donor moieties with D–π–a framing modulated electronic and nonlinear optical properties for non-fullerene-based chromophores, RSC Adv. 12 (2022) 4209–4223.
[73] E.D. Glendening, C.R. Landis, F. Weinhold, Natural bond orbital methods, Wiley Interdisc. Rev.: Computational Mol. Sci. 2 (2012) 1–42.
[74] E.D. Glendening, C.R. Landis, F. Weinhold, NBO 6.0: Natural bond orbital analysis program, J. Comput. Chem. 34 (2013) 1429–1437.
[75] M.P. Costa, L.M. Prates, L. Baptista, M.T. Cruz, I.L. Ferreira, Interaction of polyelectrolyte complex between sodium alginate and chitosan dimers with a single glyphosate molecule: a DFT and NBO study, Carbohydr. Polym. 198 (2018) 51–60.
[76] A. Lesar, I. Milošev, Density functional study of the corrosion inhibition properties of 1, 2, 4-triazole and its amino derivatives, Chem. Phys. Lett. 483 (2009) 198–203.
[77] M. Ashfaq, A. Ali, M.N. Tahir, M. Khalid, M.A. Assiri, M. Imran, K.S. Munawar, U. Habiba, Synthetic approach to achieve halo imine units: Solid-state assembly, DFT based electronic and non linear optical behavior, Chem. Phys. Lett. 803 (2022) 139843.
[78] I. Sheikhshoaie, W.M. Fabian, Quantum chemical study on the electronic structure and second-order nonlinear optical properties of salen-type Schiff bases, Dyes Pigm. 70 (2006) 91–98.
[79] C. Adant, M. Dupuis, J.L. Bredas, Ab initio study of the nonlinear optical properties of urea: Electron correlation and dispersion effects, Int. J. Quantum Chem 56 (1995) 497–507.
[80] M.F. Morks, Magnesium phosphate treatment for steel, Mater. Lett. 58 (2004) 3316–3319.
[81] A. Iwan, D. Sek, Polymers with triphenylamine units: Photonic and electroactive materials, Prog. Polym. Sci. 36 (2011) 1277–1325.
[82] S.N. Margar, N. Sekar, Nonlinear optical properties of curcumin: solvatochromism-based approach and computational study, Mol. Phys. 114 (2016) 1867–1879.
[83] M.U. Khan, M. Khalid, M. Ibrahim, A.A.C. Braga, M. Safdar, A.A. Al-Saadi, M.R.S.A. Janjua, First theoretical framework of triphenylamine–dicyanovinylene-based nonlinear optical dyes: structural modification of π-linkers, J. Phys. Chem. C 122 (2018) 4009–4018.
[84] V. Barone, M. Cossi, Quantum calculation of molecular energies and energy gradients in solution by a conductor solvent model, Chem. A Eur. J. 102 (1998) 1995–2001.